CrossMark

On the quantification of nomination feasibility in stationary gas networks with random load

Claudia Gotzes[1] · **Holger Heitsch**[2] ·
René Henrion[2] · **Rüdiger Schultz**[1]

Abstract The paper considers the computation of the probability of feasible load constellations in a stationary gas network with uncertain demand. More precisely, a network with a single entry and several exits with uncertain loads is studied. Feasibility of a load constellation is understood in the sense of an existing flow meeting these loads along with given pressure bounds in the pipes. In a first step, feasibility of deterministic exit loads is characterized algebraically and these general conditions are specified to networks involving at most one cycle. This prerequisite is essential for determining probabilities in a stochastic setting when exit loads are assumed to follow some (joint) Gaussian distribution when modeling uncertain customer demand. The key of our approach is the application of the spheric-radial decomposition of Gaussian random vectors coupled with Quasi Monte-Carlo sampling. This approach requires an efficient algorithmic treatment of the mentioned algebraic relations moreover depending on a scalar parameter. Numerical results are illustrated for different network examples and demonstrate a clear superiority in terms of precision over simple generic Monte-Carlo

✉ René Henrion
    henrion@wias-berlin.de

    Claudia Gotzes
    claudia.gotzes@uni-due.de

    Holger Heitsch
    holger.heitsch@wias-berlin.de

    Rüdiger Schultz
    ruediger.schultz@uni-due.de

[1] Faculty of Mathematics, University of Duisburg-Essen, Campus Essen, Thea-Leymann-Str. 9, 45127 Essen, Germany

[2] Weierstrass Institute, Mohrenstraße 39, 10117 Berlin, Germany

🄳 Springer

sampling. They lead to fairly accurate probability values even for moderate sample size.

Keywords Mathematical models for gas pipelines · Nomination validation · Gas network capacity · Uncertainty quantifcation · Optimization under stochastic uncertainty · Spheric-radial decomposition

Mathematics Subject Classification 62P30 · 90B15 · 90C15 · 90C31

1 Introduction

The present paper deals with mathematical aspects of gas transport in pipeline networks. The latter has been exposed to enormous deregulation in the recent past. This has created new types of economic activity, and has centered categories which had been rather marginal before. An example of the latter kind is the concept of network capacity of which the grid operator shall offer plenty in a flexible way, and this without discriminating potential market participants. Mathematically this poses the question of what capacity is and how to compute it.

Central objects of study in the present paper are gas flows in the pipes and pressures at the nodes, both under uncertainty of gas withdrawals from the network (loads) at exit (delivery) nodes. Assuming the uncertainty of withdrawals is stochastic with known distributions, an efficient method for calculating probabilities for the feasibility of load coverage is presented. Numerical tests confirm superiority of the proposed method over approaches relying on pure Monte Carlo rather than Quasi Monte Carlo sampling and/or which incorporate less structural knowledge on the (implicit) sets whose probability is looked for.

A passive steady-state network for the transport of natural gas is considered. Here, "passive" refers to the absence of controllable (or "active") network elements as there are valves, control valves, or compressors, cf. Koch et al. (2015). The network is assumed to be in steady state, i.e., time dependence of pressure and flow are neglected.

The intention behind working with passive networks in steady-state does not come from direct applicability in practice, which indeed rarely is the case. Instead, motivation comes from implanting solutions developed this way into larger models which are much closer to reality and where a probability calculation, for instance, arises as part of a functional-value or gradient calculation or approximation. At the end of the present paper some ideas in the context of chance constrained stochastic programs will be outlined.

The following two-step procedure for gas trading has been established by European legislation and illustrates the change the natural gas industry has undergone in the previous decade: First, the gas transport customer, usually so well in advance that uncertainty is present less or more massively, must *book* with a transmission system operator (TSO) capacity contracts. These are rights to inject or withdraw gas up to certain limits at corresponding nodes of the network. On the day before the booked gas transport is planned to actually take place the transport customers have to *nominate*, i.e., to declare to what extent and where they plan to exercise their rights obtained

by the booking. This procedure then allows the TSO to schedule the gas transport in advance.

The paper is organized as follows: In Sect. 2 relevant features of gas transport are introduced, consequences for mathematical modeling are discussed, and related literature is reviewed.

The basic prerequisite for determining the desired probability is the derivation of preferably explicit equalities/inequalities allowing for an efficient feasibility check of a single nomination. In Sect. 3 this will be provided both for a general network and for a tree structure.

The explicit description of feasibility enables applying a sample based estimation of the probability by means of Monte Carlo (MC) or Quasi-Monte Carlo (QMC) simulation of nominations according to the given distribution. In Sect. 4, we will consider the so-called spheric-radial decomposition of Gaussian random vectors which is tailored to multivariate Gaussian distributions and promises a significantly lower variance for the estimated probabilities.

Section 5 illustrates the application of this method for two simple examples with 3 nodes (one entry, two exits). It will be evident then, that the success of the method relies on the efficient algebraic determination of the intersection of directional rays with the set of feasible nominations. The increased difficulty by the presence of cycles in the network is highlighted.

In Sect. 6, the previous observations will be systemized towards a general application of spheric-radial decomposition to networks involving at most one cycle. Here, the general algebraic characterization derived in Sect. 3 will be exploited in a parametric fashion.

Section 7 demonstrates that the presented method provides fairly precise probabilities for cycles or trees even with comparatively large numbers of nodes. In particular the combination of QMC sampling with spheric-radial decomposition compares very favourably with simpler approaches such as MC and elementary sampling.

Finally, Sect. 8 provides some outlook of the presented methodology towards an application within optimization problems involving probabilities such as stochastic programs with probabilistic constraints. The announced outline of how to employ the present results in chance constrained stochastic programs will conclude.

2 Mathematics and gas transport: update and literature

Flow and pressure in gas grids are essentially governed by physical conservation laws. Adopting stationarity, these laws can be modeled by linear and nonlinear equations, stemming from Kirchhoff's First and Second Laws (Kirchhoff 1847) and resulting in equality systems given by multivariate polynomials of degree at most 2.

Gas flows go beyond the standard settings of network flow optimization in operations research (maximum flow, minimum cost flow, see for instance (Ahuja et al. 1993). Indeed, while flow preservation at nodes is captured by the usual linear relations, the nodal pressures are crucially ruled by the fact that the drop of their squares along a line (pipe) is proportional to the squared throughput (flow) on the line.

Gas flows are driven by potential differences. In a pipe, they are always directed towards the node with the lower potential and, due to different kinds of friction of the molecules, internal or with the pipe wall, potential, i.e., pressure, is lost. This is compensated by compressors, whose operation leads to further nonlinearities when building mathematical models.

The article (Wong and Larson 1968) might be one of the first in a vast literature that has developed in pipeline systems simulation and optimization (also consult the website www.psig.org). Of course, review of that literature is beyond the scope of the present paper, but there is an excellent up-to-date review by Ríos-Mercado and Boras-Sánchez (2015) featuring plenty of references. Furthermore there is the recent fairly comprehensive volume on evaluating capacities in gas networks (Koch et al. 2015), and also the classics (Osiadacz 1987; Zucker and Biblarz 2002) shall be mentioned at this place.

Since the deregulation of the natural gas industry, planning and operation of gas transportation are subject to new rules which are primarily determined by marketing and trading, but maintain technical feasibility an indispensable requirement. Traditional tasks such as fuel cost minimization for compressors are supplemented, if not outperformed in relevance, by feasibility and optimization problems with strong links to economics. An example for the latter is the handling of maximum pipeline capacity under strict transportation contracts.

A principal difference at the European gas market is that, formerly the gas companies have been simultaneous gas traders and network operators, whereas today there are either trading or operating companies, now acting independently without sharing knowledge.

From the position of the network operator who is responsible for reliable network operation it is mandatory that all nominations which are theoretically possible within the frame of the bookings are feasible in terms of physical, economical, and technological side conditions. The feasibility check of a nomination is called *nomination validation*, the validation of all theoretically possible nominations is referred to as *verification of booked capacities*. See Koch et al. (2015) for a detailed account on these two basic tasks in modern gas pipeline management.

Among the economical side conditions of gas network operation load coverage is of supreme importance since it reflects the very purpose of gas transmission, namely to serve customers. When quantifying coverage of future load it is obvious that uncertainty comes into play. Typically, the nature of uncertainty differs between injection points (entries), where they are more price driven, and withdrawal points (exits), where they are mainly temperature driven. This suggests to model the latter by means of random variables and to leave the former as generally uncertain. This lop-sided situation suggests to consider a probabilistic set up for exits using some probability distribution (for instance, estimated from historical data) and to impose a 'worst-case' requirement on the entry-side.

In the research literature the move to pipeline capacity driven considerations comes to the fore to bigger and bigger extent: Nomination validation is addressed in Fügenschuh et al. (2014) and Pfetsch et al. (2015). In Misra et al. (2015) throughput maximization, in Vuffray et al. (2015) robustness of natural gas flows, and in Dvi-

jotham et al. (2015) existence of optimal solutions to computationally hard problems in natural gas transmission networks are studied.

In the already mentioned article Ríos-Mercado and Boras-Sánchez (2015), Ríos-Mercado and Borraz-Sánchez conclude with research challenges from the optimization perspective caused by the need of greater flexibility in the daily gas transport operations. Among the topics they address there are (i) analogies with AC load flow in power grids, (ii) integration and solution of transient models, (iii) the need of stochastic models and approaches, and (iv) the need of analytical models for the optimization of the pipeline capacity release. The quantification of nomination feasibility in the present paper contributes to items (iii) and (iv) from that list.

3 Explicit characterization of gas flow feasibility

In a passive gas network feasibility of a nomination is equivalent to the existence of a pressure-flow profile fulfilling Kirchhoff's Laws and meeting nodal bounds on the pressure. For a characterization of the set of all capacities that can be realized, functional relations in the nomination space are sought, that hold if and only if the nomination is feasible. These functional relations become closer and closer coupled among each other the more intertwined cycles there are in the network. In what follows, a general characterization is derived that still contains as many implicit indeterminates as there are fundamental cycles in the network.

3.1 The general case

Consider a connected directed graph $G = (\mathcal{V}^+, \mathcal{E})$, with $|\mathcal{V}^+| = n + 1$ nodes and $|\mathcal{E}| = m \geq n$ edges, modeling a passive gas transportation network. Assume the network is in steady state and let $q \in \mathbb{R}^m$ denote the flows along the edges of G and $p^+ \in \mathbb{R}^{n+1}$ the pressure at nodes in $\mathcal{V}^+$. Let A^+ be the node-arc incidence matrix of G, with $a_{ie}^+ = -1$ and $a_{je}^+ = 1$ for all $i, j \in \{0, \dots, n\}$ and $e = (i, j) \in \mathcal{E}$. The vector $b^+ \in \mathbb{R}^{n+1}$ stands for a balanced load, i.e., it holds $\mathbb{1}^\top b^+ = 0$, where $\mathbb{1}$ denotes the vector of all ones in suitable dimension, here $n + 1$. Moreover, we make the sign convention that $b_i \leq 0$ at injection points (entries) and $b_i \geq 0$ at withdrawal points (exits). Mass, or mass flow, conservation at each node in $\mathcal{V}^+$ (Kirchhoff's First Law) now reads

$$A^+ q = b^+.$$

It is well-known that the matrix A^+ has rank n and that we can remove an arbitrary row without changing the solution space. Therefore, the first row $A_{0\bullet}^+$, corresponding to the node with index $i = 0$ in A^+ and the first component of $b^+ = (b_0^+, b)$ are deleted, yielding A, b and

$$Aq = b. \tag{1}$$

The pressure drop in pipe $(i, j) \in \mathcal{E}$ is modeled as

$$\left(p_i^+\right)^2 - \left(p_j^+\right)^2 = \Phi_{ij}|q_{ij}|q_{ij}$$

and for the whole network

$$\left(A^+\right)^\top \left(p^+\right)^2 = -\Phi|q|q. \tag{2}$$

Here, $\left(p^+\right)^2$ denotes the $(n+1)$-vector with components $(p_i^+)^2$, analogously, $\Phi|q|q$ has the components $\Phi_{ij}|q_{ij}|q_{ij}$ for all $(i, j) \in \mathcal{E}$. The matrix Φ is a diagonal matrix with positive entries.

It is part of our model simplification to handle Φ_{ij} as a constant and dropping in particular its dependence on pressure and flow.

With lower and upper pressure bounds p^{+min}, p^{+max} we are led to introduce the following set $\tilde{M}$ of *feasible load vectors*

$$\tilde{M} := \left\{ b^+ \,\middle|\, \mathbb{1}^\top b^+ = 0; \ \exists(q, p^+) \text{ with } p^+ \in \left[p^{+min}, p^{+max}\right] \text{ and } (1), (2) \right\}.$$

The following provides a characterization of the set $\tilde{M}$ where all pressure variables and "most of" (details below) the flow variables are eliminated. The set $\mathcal{V}$ is formed by the nodes with numbers $1, \ldots, n$.

Theorem 1 *Let $A = (A_B, A_N)$ be a partition into basis and nonbasis submatrices of A. Let Φ_B, Φ_N and q_B, q_N be according partitions of Φ and q. Let p_0 be the pressure at the node corresponding to the removed row. Define*

$$g : \mathbb{R}^{|\mathcal{V}|} \times \mathbb{R}^{|N|} \to \mathbb{R}^{|\mathcal{V}|}, \ g(u, v) := \left(A_B^\top\right)^{-1} \Phi_B \left| A_B^{-1}(u - A_N v) \right| \left(A_B^{-1}(u - A_N v)\right). \tag{3}$$

Then $\tilde{M}$ consists of all b^+ with $\mathbb{1}^\top b^+ = 0$ for which there is a z such that

$$A_N^\top g(b, z) = \Phi_N |z|z \tag{4}$$

$$(p_0^{min})^2 \leq \min_{i=1,\ldots,n} \left[(p_i^{max})^2 + g_i(b, z)\right] \tag{5}$$

$$(p_0^{max})^2 \geq \max_{i=1,\ldots,n} \left[(p_i^{min})^2 + g_i(b, z)\right] \tag{6}$$

$$\min_{i=1,\ldots,n} \left[(p_i^{max})^2 + g_i(b, z)\right] \geq \max_{i=1,\ldots,n} \left[(p_i^{min})^2 + g_i(b, z)\right] \tag{7}$$

Proof We first will show that $b^+ \in \tilde{M}$ implies the existence of some z meeting (4) to (7). Formula (1) can be written as

$$q_B = A_B^{-1}(b - A_N q_N). \tag{8}$$

Rewriting (2) yields

$$\left(A_{0B}^+\right)^\top p_0^2 + A_B^\top p^2 = -\Phi_B|q_B|q_B, \quad \left(A_{0N}^+\right)^\top p_0^2 + A_N^\top p^2 = -\Phi_N|q_N|q_N.$$

Since the rows of A^+ sum up to zero, $A_{0B}^+ = -\mathbb{1}^\top A_B$. Multiplication of the first equation with $\left(A_B^\top\right)^{-1}$ results in

$$p^2 = \mathbb{1}p_0^2 - \left(A_B^\top\right)^{-1}\Phi_B|q_B|q_B. \tag{9}$$

Inserting this into the second equation and using that $A_{0N}^+ = -\mathbb{1}^\top A_N$ provides

$$-A_N^\top \mathbb{1}p_0^2 + A_N^\top \mathbb{1}p_0^2 - A_N^\top\left(A_B^\top\right)^{-1}\Phi_B|q_B|q_B = -\Phi_N|q_N|q_N.$$

Employing (8) we obtain

$$A_N^\top\left(A_B^\top\right)^{-1}\Phi_B|A_B^{-1}(b - A_N q_N)|(A_B^{-1}(b - A_N q_N)) = \Phi_N|q_N|q_N,$$

or in terms of g,

$$A_N^\top g(b, q_N) = \Phi_N|q_N|q_N.$$

Hence, if (q, p^+) fulfills (1) and (2), then (4) is valid for $z = q_N$. Now notice that in g-notation formula (9) reads

$$p^2 = \mathbb{1}p_0^2 - g(b, q_N)$$

Of course, if $p^+ \in \left[p^{+min}, p^{+max}\right]$ then the component-wise relation also holds for the squares and the last formula provides

$$\left(p_i^{min}\right)^2 + g_i(b, q_N) \le p_0^2 \le \left(p_i^{max}\right)^2 + g_i(b, q_N) \quad \text{for all } i = 1, \dots, n.$$

Thus

$$(p_0^{min})^2 \le p_0^2 \le \min_{i=1,\dots,n}\left[(p_i^{max})^2 + g_i(b, z)\right],$$

establishing (5). Formula (6) follows in the same way, and (7) holds because, otherwise, p_0^2 would be a member of the empty set.

In the opposite direction, we show that if for some $b^+ \in \mathbb{R}^{n+1}$ with $\mathbb{1}^\top b^+ = 0$ there exists a z such that (4) to (7) are valid, then there exists (q, p^+) with $p^+ \in \left[p^{+min}, p^{+max}\right]$ fulfilling (1) and (2). Consider the two closed intervals

$$\left[\max_{i=1,\dots,n}\left[(p_i^{min})^2 + g_i(b, z)\right], \min_{i=1,\dots,n}\left[(p_i^{max})^2 + g_i(b, z)\right]\right], \left[(p_0^{min})^2, (p_0^{max})^2\right].$$

We show that their intersection is nonempty. By (7) the first interval is nonempty. If the intersection were empty then either

$$\min_{i=1,\ldots,n}\left[(p_i^{max})^2 + g_i(b,z)\right] < (p_0^{min})^2$$

or

$$(p_0^{max})^2 < \max_{i=1,\ldots,n}\left[(p_i^{min})^2 + g_i(b,z)\right].$$

Here, both outcomes produce contradictions with (5) and (6), respectively. Hence, the intersection is nonempty. Now we are in the position to make the following choices: $(p_0^{min})^2 \le p_0^2 \le (p_0^{max})^2$ and

$$p_0^2 \in \left[\max_{i=1,\ldots,n}\left[(p_i^{min})^2 + g_i(b,z)\right], \min_{i=1,\ldots,n}\left[(p_i^{max})^2 + g_i(b,z)\right]\right] \tag{10}$$

$$p_i^2 := p_0^2 - g_i(b,z) \quad \text{for all } i = 1, \ldots, n, \tag{11}$$

$$q_N := z, \tag{12}$$

$$q_B := A_B^{-1}(b - A_N z). \tag{13}$$

From (10) it follows

$$\min_{i=1,\ldots,n}\left[(p_i^{max})^2 + g_i(b,z)\right] \ge p_0^2 \ge \max_{i=1,\ldots,n}\left[(p_i^{min})^2 + g_i(b,z)\right]$$

or, equivalently,

$$(p_i^{max})^2 \ge p_0^2 - g_i(b,z) \ge (p_i^{min})^2 \quad \text{for all } i = 1, \ldots, n.$$

and, further, using (11),

$$(p_i^{max})^2 \ge p_i^2 \ge (p_i^{min})^2 \quad \text{for all } i = 1, \ldots, n.$$

This verifies the pressure bounds $p^+ \in \left[p^{+min}, p^{+max}\right]$.

In vector notation, (11) reads

$$p^2 = \mathbb{1}\,p_0^2 - g(b,z)$$

This can be continued as follows

$$A_B^\top p^2 = A_B^\top \mathbb{1}\,p_0^2 - A_B^\top g(b,z)$$
$$A_B^\top p^2 = \left(\mathbb{1}^\top A_B\right)^\top p_0^2 - \Phi_B |q_B| q_B = \left(-A_{0B}^+\right)^\top p_0^2 - \Phi_B |q_B| q_B$$
$$\left(A_{0B}^+\right)^\top p_0^2 + A_B^\top p^2 = -\Phi_B |q_B| q_B \tag{14}$$

In the first row above the equation has been multiplied by $A_B^\top$. In the second it was used that the row sum of A^+ is zero, and (14) follows. Because (4) is valid one obtains by using (12) and adding a zero term

$$-\Phi_N|q_N|q_N = -A_N^\top \mathbb{1}p_0^2 + A_N^\top \mathbb{1}p_0^2 - A_N^\top \left(A_B^\top\right)^{-1}\Phi_B|q_B|q_B.$$

With (11) this provides

$$-\Phi_N|q_N|q_N = -A_N^\top \mathbb{1}p_0^2 + A_N^\top \left(\mathbb{1}p_0^2 - \left(A_B^\top\right)^{-1}\Phi_B|q_B|q_B\right) = -A_N^\top \mathbb{1}p_0^2 + A_N^\top p^2,$$

and, again, because the rows of A^+ sum up to zero, it follows $-A_N^\top \mathbb{1} = -\left(\mathbb{1}^\top A_N\right)^\top = \left(A_{0N}^+\right)^\top$, and further

$$\left(A_{0N}^+\right)^\top p_0^2 + A_N^\top p^2 = -\Phi_N|q_N|q_N.$$

Together with (14) this yields the pressure drop Eq. (2)

$$\left(A^+\right)^\top \left(p^+\right)^2 = -\Phi|q|q.$$

It remains to show that the mass/mass flow conservation (1) holds. This follows by inserting (12) in choice (13), giving

$$q_B = A_B^{-1}(b - A_N q_N) \quad \text{which is equivalent to} \quad Aq = b.$$

Finally, since $\mathbb{1}^\top b^+ = 0$, the conservation extends to the node with index 0:

$$A_{0\bullet}^+ q = -\mathbb{1}^\top Aq = -\mathbb{1}^\top b = b_0^+.$$

This completes the proof.   □

Up to finding an auxiliary variable z satisfying (4), Theorem 1 identifies fully explicit feasibility conditions with respect to the load vector b and the side constraints (pressure bounds). Therefore, the feasibility test for b reduces to determining the (unique, for proofs see Ríos-Mercado et al. 2000; Stangl 2014) z solving (4) and then checking the inequality system (5), (6), (7). Observe that the dimension of z corresponds to the number of columns of the nonbasis part A_N of the reduced incidence matrix A, hence to the number of fundamental cycles in the network. Obviously, the situation should be particularly comfortable for networks without cycles, as is illustrated now.

3.2 Trees: connected networks without cycles

Suppose $G = (\mathcal{V}^+, \mathcal{E})$ is a tree (trivially a spanning tree of itself). Fix an arbitrary leaf node as root and number it by 0. Direct all edges in $\mathcal{E}$ away from the root. In the

incidence matrix A^+ of G delete the line corresponding to the root, yielding A which already is a basis matrix A_B so that there is no nonbasis portion A_N.

Using depth-first search, number the nodes so that numbers increase along any path from the root to one of the leaves. Then assign to any edge $(i, j) \in \mathcal{E}$ the number $\max\{i, j\}$.

Adapting a conclusion in Bertsimas and Tsitsiklis (1997), proof of Theorem 7.3, p. 281, one confirms that, rows and columns numbered that way, A_B is upper triangular. So is its inverse, for which all nonzero entries are equal to 1.

More precisely, an entry (i, j) of A_B^{-1} is 1 if and only if the unique path in G from the root to the node j contains edge number i.

For $k, \ell \in \mathcal{V}$, denote $k \succeq \ell$ if, in G, the unique directed path from the root to k, denoted $\Pi(k)$, passes through ℓ.

Since A_N is vacuous, one obtains for g as defined in (3)

$$g(b, z) = g(b) = \left(A_B^{-1}\right)^{\top} \Phi_B \left| A_B^{-1} b \right| \left(A_B^{-1} b\right)$$

and componentwise, for $k = 1, \ldots, |\mathcal{V}|$, with $h(e)$ denoting the head of edge e,

$$g_k(b) = \left[\left(A_B^{-1}\right)^{\top}\right]_{k\bullet} \Phi_B \left| A_B^{-1} b \right| \left(A_B^{-1} b\right)$$

$$= \sum_{e \in \mathcal{E}} \left[A_B^{-1}\right]_{ek} \Phi_e \left| \sum_{t \in \mathcal{V}, t \succeq h(e)} b_t \right| \left(\sum_{t \in \mathcal{V}, t \succeq h(e)} b_t \right) \tag{15}$$

$$= \sum_{e \in \Pi(k)} \Phi_e \left| \sum_{t \in \mathcal{V}, t \succeq h(e)} b_t \right| \left(\sum_{t \in \mathcal{V}, t \succeq h(e)} b_t \right). \tag{16}$$

For illustrative purposes, we will come back to trees from time to time. To reduce technicality we assume that the network has the node 0 as the only entry and all remaining nodes as exits, again with all edges directed away from 0. Then in (16) flow and edge directions conform, leading to

$$g_k(b) = \sum_{e \in \Pi(k)} \Phi_e \left(\sum_{t \in \mathcal{V}, t \succeq h(e)} b_t \right)^2. \tag{17}$$

Now, Theorem 1 specializes as follows:

Corollary 1 *If the network is a tree with a single entry as its root, then the set of feasible nominations is given by*

$$\tilde{M} = \left\{ (-\mathbb{1}^{\top}b, b) \in \mathbb{R}_- \times \mathbb{R}_+^n \middle| \begin{array}{ll} (i) & 0 \leq -\underline{y}_0 + \min_{k=1,\ldots,|\mathcal{V}|} \{\overline{y}_k + g_k(b)\} \\ (ii) & 0 \leq \overline{y}_0 - \max_{k=1,\ldots,|\mathcal{V}|} \{\underline{y}_k + g_k(b)\} \\ (iii) & 0 \leq \min_{k=1,\ldots,|\mathcal{V}|} \{\overline{y}_k + g_k(b)\} - \max_{k=1,\ldots,|\mathcal{V}|} \{\underline{y}_k + g_k(b)\} \end{array} \right\},$$

$$\tag{18}$$

where $g_k(b)$ is as in (17) and

$$\underline{y}_k := (p_k^{min})^2, \quad \overline{y}_k := (p_k^{max})^2, \quad (k = 0, \ldots, |\mathcal{V}|). \tag{19}$$

4 Random exit loads and spheric-radial decomposition of a multivariate Gaussian distribution

Next, the random nature of the exit load vector b^+ is taken into account. Since the load must be balanced, i.e., $\mathbb{1}^\top b^+ = 0$, the following set of *feasible exit load vectors* becomes relevant

$$M = \left\{ b \in \mathbb{R}^{|\mathcal{V}|} \mid (-\mathbb{1}^T b, b) \in \tilde{M} \right\}, \tag{20}$$

where $\tilde{M}$ is as in Theorem 1. More precisely, if b is identified with some random vector $\xi(\omega)$ on a probability space $(\Omega, \mathcal{A}, \mathbb{P})$, then for a given (passive) gas network (topology, pressure bounds),

$$\mathbb{P}\{\omega \in \Omega \mid \xi(\omega) \in M\}, \tag{21}$$

marks the probability of exit load vectors to be feasible.

Assume that $\xi \sim \mathcal{N}(\mu, \Sigma)$, i.e., the random vector ξ follows a multivariate Gaussian distribution with mean vector μ and positive definite covariance matrix Σ. Behind this choice there are the following reasons:

The main variation of exit load data is temperature driven. However, even at fixed temperature, considerable random variation remains. That is why exit loads can be understood as a stochastic process depending on temperature and may be characterized by a finite family of multivariate distributions, each of them referring to some (rather narrow) range of temperature and reflecting the joint distribution of loads at the given set of exit points, see Koch et al. (2015, Chapter 13). As recorded in the same reference (Koch et al. 2015, Table 13.3), these distributions are most likely to be Gaussian (possibly truncated) or lognormal. Our assumption to consider a multivariate Gaussian distribution for ξ can therefore be seen as a prototype setting which—using the spheric-radial decomposition presented next—maybe adapted without much effort to more realistic settings (multivariate log-normal distributions, probabilities with respect to several temperature classes simultaneously, etc.).

4.1 Spheric-radial decomposition

Returning to (21), the computation of this probability amounts to the solution of a possibly highdimensional (number of exit nodes) multiple integral. A favourable situation to carry out this computation under Gaussian distribution occurs for polyhedral sets M. For details, we refer to Genz and Bretz (2009), which not only gives an excellent overview on this topic but also presents a very efficient algorithm developed by the author himself. Unfortunately, in the setting of Theorem 1 we cannot expect the feasible

set to be polyhedral, not even convex. Therefore, recourse to the mentioned algorithm is not possible. Still one could resort to Monte Carlo (MC) or Quasi-Monte Carlo (QMC) simulations of ξ and exploit the relations provided in Theorem 1 in order to approximate the desired probability directly. We shall rather propose here the so-called *spheric-radial decomposition* of a Gaussian distribution (e.g., Deák 2000) as a promising alternative which not only may significantly reduce the variance of estimating (21) but moreover offers the possibility of efficiently approximating gradients of (21) with respect to an external parameter. This last feature is of supreme importance for optimization problems under probabilistic constraints. The following result is well-known:

Theorem 2 (spheric-radial decomposition) *Let $\xi \sim \mathcal{N}(0, R)$ be some n-dimensional standard Gaussian distribution with zero mean and positive definite correlation matrix R. Then, for any Borel measurable subset $M \subseteq \mathbb{R}^n$ it holds that*

$$\mathbb{P}(\xi \in M) = \int_{\mathbb{S}^{n-1}} \mu_\chi\{r \geq 0 \,|\, rLv \in M\} d\mu_\eta(v),$$

where $\mathbb{S}^{n-1}$ is the $(n-1)$-dimensional sphere in $\mathbb{R}^n$, μ_η is the uniform distribution on $\mathbb{S}^{n-1}$, μ_χ denotes the χ-distribution with n degrees of freedom and L is such that $R = LL^T$ (e.g., Cholesky decomposition).

To make this result available to the present analysis, it has to be adapted to general Gaussian distributions $\xi \sim \mathcal{N}(\mu, \Sigma)$. This is done by passing to the standardized random vector

$$\xi^* := D^{-1}(\xi - \mu) \sim \mathcal{N}(0, R); \quad D := \text{diag}\,(\sqrt{\Sigma_{ii}})_{i=1,\ldots,n}; \quad R := D^{-1}\Sigma D^{-1}$$

and observing that $\mathbb{P}(\xi \in M) = \mathbb{P}(\xi^* \in D^{-1}(M - \mu))$. Now, to compute $\mathbb{P}(\xi \in M)$, Theorem 2 has to be applied to $\mathbb{P}(\xi^* \in M^*)$ for $M^* := D^{-1}(M - \mu)$.

The previous observations suggest the following conceptual algorithm to approximate the Gaussian probability of a set M:

Algorithm 3 Let $\xi \sim \mathcal{N}(\mu, \Sigma)$ and L such that $LL^T = \Sigma$ (e.g., Cholesky factorization).

1. Sample N points $\{v_1, \ldots, v_N\}$ uniformly distributed on the sphere $\mathbb{S}^{n-1}$.
2. Compute the one-dimensional sets $M_i := \{r \geq 0 \,|\, rLv_i + \mu \in M\}$ for $i = 1, \ldots, N$.
3. Set $\mathbb{P}(\xi \in M) \approx N^{-1} \sum_{i=1}^{N} \mu_\chi(M_i)$.

The simplest way to carry out the first step of the algorithm consists in MC sampling of the standard Gaussian distribution $\mathcal{N}(0, I_n)$ and then normalizing the obtained sampling points to unit length. This is well-known to provide a sample of the uniform distribution on the sphere. It is significantly more efficient, however, to replace MC sampling by QMC sampling of the same standard Gaussian distribution. This will be the method of choice for this paper. An additional increase of efficiency might be expected from applying QMC sampling directly tailored to the sphere (Brauchart et al. 2014).

The second step is at the heart of the algorithm and requires structural knowledge about the set M. In the simplest case (e.g., if M is convex) the sets M_i are one-dimensional intervals. Figure 2 in Sect. 5.1 shows an example of sampling points v_1, v_2, v_3, v_4 such that all sets M_i are intervals of the form $[0, r_i]$. In more complex situations, the M_i may be finite unions of intervals whose endpoints have to be determined, for instance, as zeros of some higher order polynomial.

The last step consists in determining the probabilities of the sets M_i with respect to the χ-distribution and in calculating the average over all samples. Note, that the χ-probabilities are easily evaluated using numerically highly precise standard approximations for the distribution function F_χ of this one-dimensional distribution. If, for instance,

$$M_i = \cup_{j=1}^{l} [a_j, b_j]$$

is a finite and disjoint union of intervals, then

$$\mu_\chi(M_i) = \sum_{j=1}^{l} (F_\chi(b_j) - F_\chi(a_j)).$$

4.2 Application to tree structured networks

As shown in Corollary 1, the representation of feasibility of nominations becomes handy if there are no cycles in the network G. This will be discussed now, while the more involved case of a cycle will be addressed in Sect. 6.

Given a vector $v_i \in \mathbb{S}^{n-1}$ sampled in Step 1 of Algorithm 3, the crucial Step 2, consists in representing the set $M_i := \{r \geq 0 \mid rLv_i + \mu \in M\}$ as a union of disjoint intervals. Setting $w := Lv_i$ and $b(r) := rw + \mu$, we obtain from (16), (18) and (20) that

$$M_i =$$

$$\left\{ r \geq 0 \left| \begin{array}{ll} \text{(i)} & 0 \leq rw + \mu \\ \text{(ii)} & 0 \leq -(p_0^{min})^2 + \min_{k=1,\ldots,|\mathcal{V}|} \left[(p_k^{max})^2 + h_k(r) \right] \\ \text{(iii)} & 0 \leq (p_0^{max})^2 - \max_{k=1,\ldots,|\mathcal{V}|} \left[(p_k^{min})^2 + h_k(r) \right] \\ \text{(iv)} & 0 \leq \min_{k=1,\ldots,|\mathcal{V}|} \left[(p_k^{max})^2 + h_k(r) \right] - \max_{k=1,\ldots,|\mathcal{V}|} \left[(p_k^{min})^2 + h_k(r) \right] \end{array} \right. \right\},$$

$$(22)$$

where

$$h_k(r) := g_k(b(r)) = \sum_{e \in \Pi(k)} \Phi_e \left(\sum_{t \in \mathcal{V}, t \geq h(e)} (rw_t + \mu_t) \right)^2 \quad (k = 1, \ldots, |\mathcal{V}|). \quad (23)$$

Note that (i) in (22) determines the interval, for which $b(r)$ is nonnegative. Later we will refer to it as *regular range*. The remaining conditions (ii–iv), however, can be written as system of quadratic inequalities only, because $h_k(r)$ is quadratic in r for all k due to (23). In particular, we may write

$$M_i = \left\{ r \geq 0 \,\middle|\, 0 \leq p^{(j)}(r) \quad (j = 1, \ldots, s) \right\},$$

where the $p^{(j)}(r)$ are (multivariate) polynomials of maximum degree 2 and the index j is running from 1 to s according to the number of inequalities appearing in (22). Thus, each inequality $0 \leq p^{(j)}(r)$ represents a union of at most two disjoint intervals whose limits are determined in an elementary way. Then, M_i—as an intersection of such sets—can be easily represented itself as a finite union of disjoint intervals as required for Step 3 of Algorithm 3 (see discussion at the end of Sect. 4.1).

5 Illustrative examples

In order to illustrate the set M of feasible exit load vectors, two examples of elementary networks, namely tree and cycle, are presented.

5.1 Simple tree

Consider the simple tree of Fig. 1 with one entry and two exit nodes. Figure 1 displays the directed graph and flows corresponding to the given network. Recalling (20), and applying relations (17), (18) one obtains

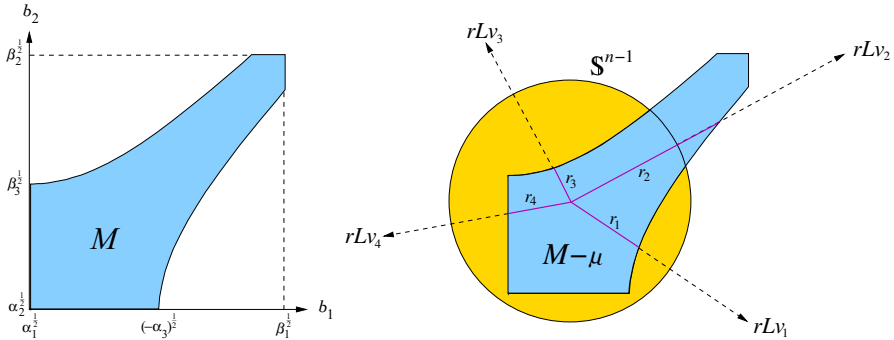**Fig. 1** Simple tree with one entry node (0) and two exit nodes (1, 2)
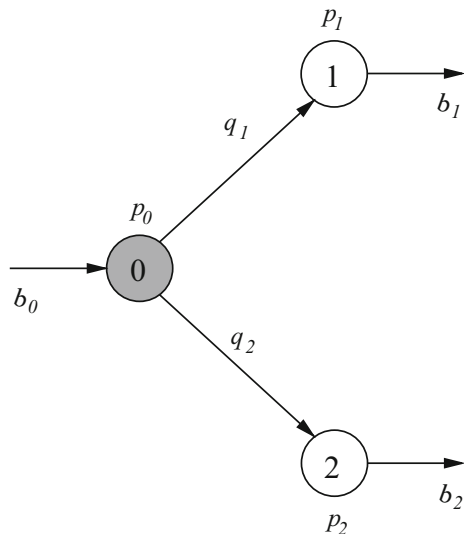
Fig. 2 Shape of the set M of feasible exit nodes (*left*) and its centered versions $M - \mu$ along with illustration of spherical-radial decomposition (*right*) for a special setting of pressure bounds

$$M = \left\{ b \in \mathbb{R}^2_+ \left| \begin{array}{l} 0 \leq -\underline{y}_0 + \min\{\overline{y}_1 + \phi_1 b_1^2, \ \overline{y}_2 + \phi_2 b_2^2\} \\ 0 \leq \ \ \overline{y}_0 - \max\{\underline{y}_1 + \phi_1 b_1^2, \ \underline{y}_2 + \phi_2 b_2^2\} \\ 0 \leq \ \ \overline{y}_1 + \phi_1 b_1^2 - \underline{y}_2 - \phi_2 b_2^2 \\ 0 \leq \ \ \overline{y}_2 + \phi_2 b_2^2 - \underline{y}_1 - \phi_1 b_1^2 \end{array} \right. \right\}. \tag{24}$$

For simplicity we put $\phi_1 := \phi_2 := 1$, introduce the short hand notation

$$\alpha_1 := \underline{y}_0 - \overline{y}_1; \ \ \alpha_2 := \underline{y}_0 - \overline{y}_2; \ \ \alpha_3 := \underline{y}_1 - \overline{y}_2$$
$$\beta_1 := \overline{y}_0 - \underline{y}_1; \ \ \beta_2 := \overline{y}_0 - \underline{y}_2; \ \ \beta_3 := \overline{y}_1 - \underline{y}_2$$

and derive that

$$M = \left\{ b \in \mathbb{R}^2_+ \left| \begin{array}{ll} \text{(i)} & \alpha_1 \leq b_1^2 \leq \beta_1 \\ \text{(ii)} & \alpha_2 \leq b_2^2 \leq \beta_2 \\ \text{(iii)} & \alpha_3 \leq b_2^2 - b_1^2 \leq \beta_3 \end{array} \right. \right\}.$$

Figure 2 (left) illustrates the set M of feasible pairs (b_1, b_2) of exit nodes for assumed pressure bounds

$$[\underline{y}_0, \overline{y}_0] = [2, 5], \quad [\underline{y}_1, \overline{y}_1] = [\underline{y}_2, \overline{y}_2] = [1, 2]$$

implying that $\alpha_1 = 0$, $\alpha_2 = 0$, $\alpha_3 = -1$, $\beta_1 = 4$, $\beta_2 = 4$, $\beta_3 = 1$. As can be seen, the set M cannot be expected to be convex in general.

Figure 2 (right) illustrates the shifted set $M - \mu$ needed in Step 2 of Algorithm 3 when determining the Gaussian probability of M under distribution $b \sim \mathcal{N}(\mu, \Sigma)$ of the random exit load vector. Here, we have assumed that $\Sigma = I_2$ and $\mu = (0.5, 0.8)$,

Fig. 3 Simple cycle with one
entry node (0) and two exit
nodes (1, 2)
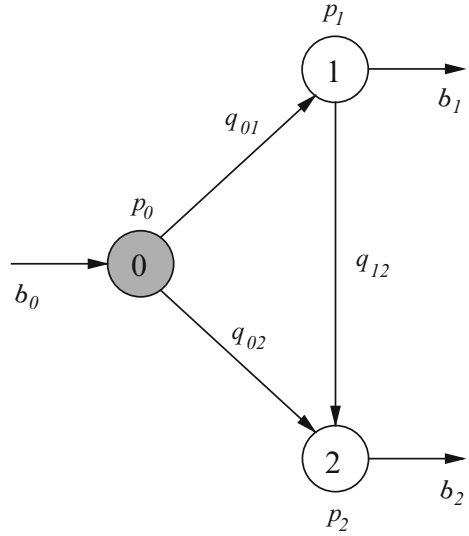
so that the mean load vector is feasible. In this case $L = I_2$ and the sets M_i defined
in Algorithm 3 reduce to intervals $[0, r_i]$ (illustrated in Fig. 2 (right) for a set of four
sample points v_i from the sphere).

5.2 Simple cycle

To illustrate the difficulty in contrast to a tree, the elementary cycle depicted in Fig. 3
is considered next. Now, for a description of the set of feasible exit loads, Corollary 1
no longer applies and resorting to Theorem 1 is the option of choice. With the notation
introduced there, the incidence matrix reads

$$A^+ = \left(\begin{array}{cc|c} -1 & -1 & 0 \\ 1 & 0 & -1 \\ 0 & 1 & 1 \end{array} \right) = \left(\begin{array}{c|c} -1 \quad -1 & 0 \\ \hline A_B & A_N \end{array} \right)$$

With $A_B = I$, $A_N = (-1, 1)^T$ and ϕ_i corresponding to the edge in the i-th column
of A^+, the components g_i of the mapping g from Theorem 1 become

$$g_1(b, z) = \phi_1(b_1 + z)|b_1 + z|,$$
$$g_2(b, z) = \phi_2(b_2 - z)|b_2 - z|.$$

Recalling (19) and (20), relations (4), (5), (6), (7) yield the characterization

$$
M = \left\{ b \in \mathbb{R}_+^2 \; \middle| \; \exists z : \begin{array}{l}
0 = \phi_1 |b_1 + z|(b_1 + z) - \phi_2 |b_2 - z|(b_2 - z) + \phi_3 |z|z \\
0 \leq -\underline{y}_0 + \overline{y}_1 + \phi_1 |b_1 + z|(b_1 + z) \\
0 \leq -\underline{y}_0 + \overline{y}_2 + \phi_2 |b_2 - z|(b_2 - z) \\
0 \leq \quad \overline{y}_0 - \underline{y}_1 - \phi_1 |b_1 + z|(b_1 + z) \\
0 \leq \quad \overline{y}_0 - \underline{y}_2 - \phi_2 |b_2 - z|(b_2 - z) \\
0 \leq \overline{y}_1 + \phi_1 |b_1 + z|(b_1 + z) - \underline{y}_2 + \phi_2 |b_2 - z|(b_2 - z) \\
0 \leq \overline{y}_2 + \phi_2 |b_2 - z|(b_2 - z) - \underline{y}_1 + \phi_1 |b_1 + z|(b_1 + z)
\end{array} \right\} .
$$

$$(25)$$

The difficulty here is the implicit dependence on the variable z. To eliminate this variable one solves

$$\phi_1 |b_1 + z|(b_1 + z) - \phi_2 |b_2 - z|(b_2 - z) + \phi_3 |z|z = 0. \tag{26}$$

The absolute values require a case distinction, producing a quadratic equation in z for every individual case. The root formula for quadratic equations in one variable yields explicit representations of z by the load components b_i.

The network at hand being small and, setting once more $\phi_1 = \phi_2 = \phi_3 = 1$, symmetric, a substantial (but exceptional) short cut (avoiding a more elaborate case distinction) is possible. Indeed, observing that, since considered loads, it holds that $b_1 \geq 0, b_2 \geq 0$. Imposing $b_2 \geq b_1$ then implies the pressure at node 2 to be less than or equal to that at node 1, thus the flow is going from node 1 to 2, and $z \geq 0$. Analogously, $b_1 \geq b_2$ implies $z \leq 0$.

With $z \geq 0$ equation (26) becomes

$$|b_2 - z|(b_2 - z) = (b_1 + z)^2 + z^2$$

It follows that the left-hand side has to be nonnegative, and the equation reads

$$(b_2 - z)^2 = (b_1 + z)^2 + z^2.$$

Analogously, with $z \leq 0$, or equivalently $b_1 \leq b_2$ the following equation results

$$(b_1 + z)^2 = (b_2 - z)^2 + z^2$$

Solving these equations leads to

$$
z = \begin{cases}
-b_1 - b_2 + \sqrt{2(b_2^2 + b_1 b_2)} \geq 0 & \text{if } b_2 \geq b_1, \\
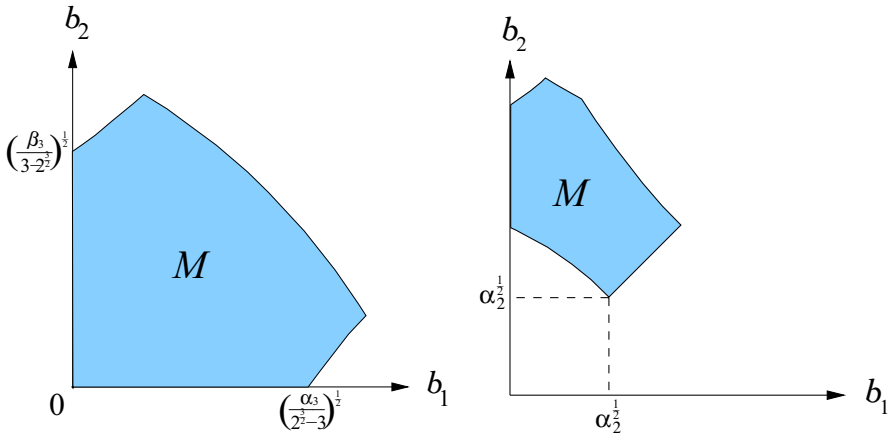b_1 + b_2 - \sqrt{2(b_1^2 + b_1 b_2)} < 0 & \text{otherwise.}
\end{cases}
$$

Fig. 4 Shape of the feasible set M for two different pressure bound settings

This permits to eliminate z in (25):

$$
\begin{aligned}
h_1(b_1, b_2) &:= |b_1 + z|(b_1 + z) = (b_1 + z)^2 \\
&= \begin{cases}
\left(\sqrt{2(b_2^2 + b_1 b_2)} - b_2\right)^2 & \text{if } b_2 \geq b_1, \\
\left(2b_1 + b_2 - \sqrt{2(b_1^2 + b_1 b_2)}\right)^2 & \text{otherwise,}
\end{cases} \\
h_2(b_1, b_2) &:= |b_2 - z|(b_2 - z) = (b_2 - z)^2 \\
&= \begin{cases}
\left(2b_2 + b_1 - \sqrt{2(b_2^2 + b_1 b_2)}\right)^2 & \text{if } b_2 \geq b_1, \\
\left(\sqrt{2(b_1^2 + b_1 b_2)} - b_1\right)^2 & \text{otherwise,}
\end{cases}
\end{aligned}
$$

and arrive at a representation of feasibility in the space of load vectors b:

$$
M = \left\{ b \in \mathbb{R}_+^2 \;\middle|\;
\begin{array}{ll}
\text{(i)} & \alpha_1 \leq h_1(b_1, b_2) \leq \beta_1 \\
\text{(ii)} & \alpha_2 \leq h_2(b_1, b_2) \leq \beta_2 \\
\text{(iii)} & \alpha_3 \leq h_2(b_1, b_2) - h_1(b_1, b_2) \leq \beta_3
\end{array}
\right\},
$$

where we used the same notation α_i, β_i as in the previous example.

Figure 4 illustrates the set of feasible exit load vectors for the same pressure bound setting as in the tree example in Sect. 5.1 (left) and for a different setting (right).

6 Feasibility of exit loads in a cycle with a single entry

As could be seen from the previous examples, dealing with cycles inside the network increases the amount of numerical work in order to check whether a concrete exit load scenario is feasible or not, while the same question is more or less evident for a tree

thanks to Corollary 1. In this section, we present a systematic algorithmic approach for making relations (4), (5), (6), (7) explicit for a network consisting of a single loop with a single entry. At the same time, this approach shall be adapted to the sampling step in the spheric-radial decomposition in order to finally allow a fairly precise computation of the desired probability $\mathbb{P}(\xi \in M)$.

6.1 Algebraic representation of the feasibility set

We assume that the cycle contains $|\mathcal{V}^+| = n+1$ nodes where node 0 represents the only entry. For analytical reasons, we label the edges according to their order when running through the cycle in opposite direction to the nonbasis edge. Then, the $(n+1, n+1)$-incidence matrix of this network is partitioned as follows:

$$
A^+ = \left(
\begin{array}{cccc|c}
-1 & & & & -1 \\
1 & -1 & & & \\
& 1 & \ddots & & \\
& & \ddots & -1 & \\
& & & 1 & 1
\end{array}
\right).
\tag{27}
$$

A special instance of such cycle with its incidence matrix is provided in Sect. 7. Given the partition above, the basis and nonbasis submatrices of A^+ take the form

$$
A_B = \left(
\begin{array}{cccc}
1 & -1 & & \\
& 1 & \ddots & \\
& & \ddots & -1 \\
& & & 1
\end{array}
\right), \quad
A_B^{-1} = \left(
\begin{array}{cccc}
1 & 1 & \cdots & 1 \\
& 1 & \ddots & \vdots \\
& & \ddots & 1 \\
& & & 1
\end{array}
\right) \quad \text{and} \quad
A_N = \left(
\begin{array}{c}
0 \\
\vdots \\
0 \\
1
\end{array}
\right).
\tag{28}
$$

In order to decide whether an exit load vector b is feasible or not, we, first of all, have to solve the Eq. (4) for the variable z. Moreover, with regard to the spheric-radial decomposition approach we need to determine an explicit function $z(\cdot)$ describing the dependence of z on b. To this end, for a given vector b, we define recursively the quantities

$$
\beta_{n+1} := 0, \quad \beta_k := \beta_{k+1} + b_k \quad \text{for} \quad k = n, \ldots, 1,
\tag{29}
$$

and state the following result:

Proposition 1 *Given the incidence matrix* (27), (4) *is equivalent to the equation*

$$
f_A(z) := \phi_1 |\beta_1 - z|^* + \cdots + \phi_{n+1} |\beta_{n+1} - z|^* = 0,
\tag{30}
$$

where $\phi_k := \Phi_{k-1,k}$ $(k = 1, \ldots, n)$, $\phi_{n+1} := \Phi_{0n}$ *and* $|x|^* := |x|x$. *Moreover,* f_A *is strictly monotonically decreasing, there exists a unique* z^* *with* $f_A(z^*) = 0$ *and it holds that* $\beta_{n+1} \leq z^* \leq \beta_1$.

Proof Observe that, by (28),

$$
|A_B^{-1}(b - A_N z)|^* =
\begin{vmatrix}
b_1 + b_2 + \cdots + b_n - z \\
b_2 + \cdots + b_n - z \\
\ddots \\
b_n - z
\end{vmatrix}^*
=
\begin{vmatrix}
\beta_1 - z \\
\beta_2 - z \\
\vdots \\
\beta_n - z
\end{vmatrix}^* .
$$

Moreover, with (28) we have that

$$
g_i(b, z) = \sum_{j=1}^{i} \phi_j |\beta_j - z|^* \quad (i = 1, \ldots, n). \tag{31}
$$

The submatrix $\Phi_N = \Phi_{0n} = \phi_{n+1}$ is a scalar coefficient corresponding to edge $(0, n) \in \mathcal{E}$. Therefore, recalling that $\beta_{n+1} = 0$ by definition, we arrive at

$$
A_N^T g(b, z) - \Phi_N |z|^* = g_n(b, z) + \phi_{n+1} |\beta_{n+1} - z|^* = \sum_{j=1}^{n+1} \phi_j |\beta_j - z|^* .
$$

This implies (30). Next, by $\phi_k > 0$, each of the functions $\phi_k |\beta_k - z|^*$ has a nonpositive derivative vanishing exactly at $z = \beta_k$. Hence, these functions are strictly monotonically decreasing and so is f_A as their sum. Finally, the sequence β_k is decreasing too by definition and due to $b_k \geq 0$. This entails that $f_A(\beta_1) \leq 0$ and $f_A(\beta_{n+1}) \geq 0$. Since f_A is strictly decreasing, there exists a unique z^* with $f_A(z^*) = 0$ and it holds that $\beta_{n+1} \leq z^* \leq \beta_1$. □

Proposition 1 provides an algorithmic approach to solve $f_A(z) = 0$, analytically. Determining the index k^* such that $z^* \in [\beta_{k^*+1}, \beta_{k^*}]$ allows us to eliminate the absolute value in the representation (30) of f_A and to compute z^* as the square root of a scalar quadratic function. To identify the index k^*, we make use of the property

$$
f_A(\beta_1) \leq f_A(\beta_2) \leq \cdots \leq f_A(\beta_{n+1}).
$$

Since $f_A(\beta_1) \leq 0$ and $f_A(\beta_{n+1}) \geq 0$ we just need to track the sign of function values in the above sequence and get the index k^* as the one with $f_A(\beta_{k^*}) \leq 0$ and $f_A(\beta_{k^*+1}) \geq 0$. Then z^* is the (unique) solution of the quadratic equation

$$
\sum_{i=1}^{k*} \phi_i (\beta_i - z)^2 - \sum_{i=k^*+1}^{n+1} \phi_i (\beta_i - z)^2 = 0, \quad z \in [\beta_{k^*+1}, \beta_{k^*}] \tag{32}
$$

in the indicated interval. In order to emphasize the dependence of this solution on b (which will be needed later for applying the spheric-radial decomposition approach), we shall denote the parametric solution of (32) by $z(b)$. By doing so, Theorem 1 and

(20) yield that an exit load vector b in the given cycle with single entry at node 0 belongs to the set M if and only if

$$0 \leq -(p_0^{min})^2 + \min_{i=1,\ldots,n} \left[(p_i^{max})^2 + g_i(b, z(b)) \right], \tag{33}$$

$$0 \leq (p_0^{max})^2 - \max_{i=1,\ldots,n} \left[(p_i^{min})^2 + g_i(b, z(b)) \right], \tag{34}$$

$$0 \leq \min_{i=1,\ldots,n} \left[(p_i^{max})^2 + g_i(b, z(b)) \right] - \max_{i=1,\ldots,n} \left[(p_i^{min})^2 + g_i(b, z(b)) \right], \tag{35}$$

where the g_i are defined in (31).

6.2 Application to spheric-radial decomposition

Our goal now is to exploit the results for characterizing the set M in case of a cycle, in order to efficiently compute its probability under uncertain exit loads via spheric-radial decomposition as made precise in Algorithm 3. As mentioned earlier, the crucial step of Algorithm 3 (Step 2) consists in determining the one-dimensional set

$$R_{\text{feas}} := \{r \geq 0 \,|\, rw + \mu \in M\}. \tag{36}$$

where $w := Lv_i$ for given matrix L such that $LL^T = \Sigma$, for given (mean) vector μ and given sample $v_i \in \mathbb{S}^{n-1}$. Note that L is regular because the covariance matrix Σ was required to be positive definite. Hence, $w \neq 0$, because otherwise the contradiction $v_i = 0$ to $v_i \in \mathbb{S}^{n-1}$ would result. Clearly, the role of b in the question '$b \in M$?' answered in the previous section, will be taken now by the vector $b(r) := rw + \mu$. first of all, the range of feasible $r \geq 0$ is constrained by the fact that exit loads are nonnegative. This leads us to define a *regular range*

$$R_{\text{reg}} := \{r \geq 0 \,|\, rw + \mu \geq 0\} \supseteq R_{\text{feas}}. \tag{37}$$

The regular range represents an interval $R_{\text{reg}} = [\underline{r}, \overline{r}]$ in $\mathbb{R}$. Now, (33), (34), (35), applied to $b(r)$ rather than to the fixed b yield

$$R_{\text{feas}}$$
$$= \left\{ r \in [\underline{r}, \overline{r}] \,\middle|\, \begin{array}{ll} \text{(i)} & 0 \leq -(p_0^{min})^2 + \min_{i=1,\ldots,n} \left[(p_i^{max})^2 + h_i(r) \right] \\[2mm] \text{(ii)} & 0 \leq (p_0^{max})^2 - \max_{i=1,\ldots,n} \left[(p_i^{min})^2 + h_i(r) \right] \\[2mm] \text{(iii)} & 0 \leq \min_{i=1,\ldots,n} \left[(p_i^{max})^2 + h_i(r) \right] - \max_{i=1,\ldots,n} \left[(p_i^{min})^2 + h_i(r) \right] \end{array} \right\}, \tag{38}$$

where, with the definition $\tilde{z}(r) := z(b(r))$, we put

$$h_i(r) := g_i(b(r), \tilde{z}(r)) \quad (i = 1, \ldots, n). \tag{39}$$

In the following, our aim is to determine the one-dimensional set R_{feas} as a finite union

$$R_{\text{feas}} = \cup_{j=1}^{l}[a_j, b_j] \tag{40}$$

of disjoint intervals as discussed in Sect. 4, in order to compute the χ-probabilities $\mu_\chi(M_i)$ in Step 3. of Algorithm 3.

Two steps will be required to achieve this goal: first, we have to find an analytic expression for the function $\tilde{z}$ in (39), which we will refer to as the *outer problem*. Second, given this analytic expression, we have to identify the representation (40), which we will refer to as the *inner problem*.

6.2.1 The outer problem

The outer problem consists in determining the roots of function f_A given in (30), but now for parameters $\beta_1, \ldots, \beta_{n+1}$ depending on r. More precisely, for the r-dependent vectors $b(r) = rw + \mu$, we may define the sequence of β-values analogously to (29):

$$\beta_{n+1}(r) := 0, \quad \beta_k(r) = \beta_{k+1}(r) + rw_k + \mu_k \quad \text{for} \quad k = 1, \ldots, n. \tag{41}$$

As before, monotonicity is maintained:

$$0 = \beta_{n+1}(r) \le \beta_n(r) \le \cdots \le \beta_1(r) \quad \forall r \in [\underline{r}, \overline{r}]. \tag{42}$$

Therefore, we can apply the results of the previous Sect. 6.1 for any $r \in [\underline{r}, \overline{r}]$. Summarizing, in order to solve (30) we have to solve

$$\tilde{f}_A(z, r) := \phi_1|\beta_1(r) - z|^* + \cdots + \phi_{n+1}|\beta_{n+1}(r) - z|^* = 0 \tag{43}$$

for z parametrically in $r \in [\underline{r}, \overline{r}]$. The solution function will be called $\tilde{z}(r)$ and corresponds to $z(b(r))$ with respect to the parametric solution $z(b)$ of (32).

Theorem 4 *There exists a uniquely defined and continuous function $\tilde{z} : [\underline{r}, \overline{r}] \to \mathbb{R}$ such that $\tilde{f}_A(\tilde{z}(r), r) = 0$ for all $r \in [\underline{r}, \overline{r}]$. Moreover, there are numbers $r_1, \ldots r_t$ and indices $k_1, \ldots, k_t$ such that*

$$r_0 =: \underline{r} \le r_1 \le \cdots \le r_{t-1} \le r_t := \overline{r} \quad and$$

$$\tilde{z}(r) \in [\beta_{k_j+1}(r), \beta_{k_j}(r)] \quad \forall r \in [r_{j-1}, r_j] \quad (j = 1, \ldots, t). \tag{44}$$

The solution function $\tilde{z}$ is of the form

$$\tilde{z}(r) = \begin{cases} -\frac{1}{2c}\left(\ell(r) + \sqrt{\ell^2(r) - 4cq(r)}\right) & \text{if } c > 0, \\ -\frac{1}{2c}\left(\ell(r) - \sqrt{\ell^2(r) - 4cq(r)}\right) & \text{if } c < 0 \quad \forall r \in [r_{j-1}, r_j] \\ -\frac{q(r)}{\ell(r)}, & \text{if } c = 0 \end{cases} \tag{45}$$

$(j = 1, \ldots, t)$, *where* $\ell(r)$ *and* $q(r)$ *are well-defined affine linear and quadratic functions, respectively, and, the constant* c *is given by* $c = \sum_{k=1}^{k_j} \phi_k - \sum_{k=k_j+1}^{n+1} \phi_k$.

Proof Existence and uniqueness of the function $\tilde{z}(r)$ follow from Proposition 1 for any fixed $r \in [\underline{r}, \overline{r}]$. Concerning continuity of $\tilde{z}$, observe first that $\tilde{f}_A$ is continuously differentiable with

$$\frac{\partial \tilde{f}_A}{\partial z}(z, r) = 2 \sum_{j=1}^{j(z,r)} \phi_j (\beta_j(r) - z) - 2 \sum_{j=j(z,r)+1}^{n+1} \phi_j (\beta_j(r) - z) \leq 0$$
$$\forall r \in [\underline{r}, \overline{r}] \, \forall z \in \mathbb{R},$$

where $j(z, r)$ refers to the largest integer j such that $\beta_j(r) \leq z$. Clearly, the partial derivative above is zero at some $r^* \in [\underline{r}, \overline{r}]$ if and only if $z = \beta_1(r^*) = \cdots = \beta_{n+1}(r^*)$. Assume in such case that $r^* \in (\underline{r}, \overline{r})$. Note that $\beta_{n+1} \equiv 0$ by (41). On the other hand, again by (41),

$$\beta_k(r) = r(w_k + \cdots + w_n) + (\mu_k + \cdots + \mu_n) \quad (k = 1, \ldots, n). \tag{46}$$

If the slopes $w_k + \cdots + w_n$ of all these affine linear functions were zero, then the contradiction $w = 0$ would follow. Hence, there is some $k \in \{1, \ldots, n\}$ such that the slope of β_k is different from zero. From $\beta_k(r^*) = \beta_{n+1}(r^*) = 0$ it therefore follows that $\beta_k(r') < 0$ for certain r' arbitrarily close to r^*. In particular, we may assume that $r' \in (\underline{r}, \overline{r})$ which contradicts (42). Consequently, the assumption $r^* \in (\underline{r}, \overline{r})$ was wrong and we infer that

$$\frac{\partial \tilde{f}_A}{\partial z}(z, r) < 0 \quad \forall r \in (\underline{r}, \overline{r}) \quad \forall z \in \mathbb{R}.$$

Hence, the implicit function theorem yields that $\tilde{z}$ is continuous on $(\underline{r}, \overline{r})$ and it can have a discontinuity at $r^* \in \{\underline{r}, \overline{r}\}$ only if $z = \beta_1(r^*) = \cdots = \beta_{n+1}(r^*) = 0$. Then, $\tilde{z}(r^*) = 0$ by (43). On the other hand, Proposition 1 implies that $\beta_{n+1}(r) \leq \tilde{z}(r) \leq \beta_1(r)$ for all $r \in [\underline{r}, \overline{r}]$. Hence, continuity of β_1, β_{n+1} yields that

$$\lim_{r \to r^*} \tilde{z}(r) = \beta_{n+1}(r^*) = 0 = \tilde{z}(r^*).$$

This, however, is continuity of $\tilde{z}$ at $r^* \in \{\underline{r}, \overline{r}\}$. Summarizing, $\tilde{z}$ is continuous on the whole interval $[\underline{r}, \overline{r}]$ as asserted.

Next, we want to prove (44). Clearly, for every fixed r, $\tilde{z}(r)$ meets a certain interval $[\beta_{k+1}(r), \beta_k(r)]$, where $k \in \{1, \ldots, n\}$. Due to continuity of both $\tilde{z}$ and the interval limits, this index k can only change for some r with $\tilde{z}(r) = \beta_{k+1}(r)$ or $\tilde{z}(r) = \beta_k(r)$. All such points are contained in the set

$$S := \{r \in \mathbb{R} \mid \exists k \in \{1, \ldots, n+1\} : \tilde{f}_A(\beta_k(r), r) = 0\}. \tag{47}$$

We note that $\tilde{f}_A(\beta_k(r), r)$ is a quadratic function in r for any $k \in \{1, \ldots, n+1\}$. We distinguish two cases: first, assume that there exists some $k \in \{1, \ldots, n+1\}$ such that $\tilde{f}_A(\beta_k(r), r) = 0$ for all $r \in [\underline{r}, \overline{r}]$. Then, $\tilde{z}(r) = \beta_k(r)$ for all $r \in [\underline{r}, \overline{r}]$ and we get the representation (44) by choosing $t := 1$ and $k_1 := k$ if $k \leq n$ and $k_1 := n$ if $k = n+1$. Otherwise, all quadratic functions $\tilde{f}_A(\beta_k(r), r)$ are not identically zero and thus have at most two roots. Thus, the set S is finite and we may order its elements such that

$$S \cap [\underline{r}, \overline{r}] = \{r_1, \ldots, r_{t-1}\}, \quad \text{where } r_1 \leq \cdots \leq r_{t-1}.$$

Setting $r_0 := \underline{r}$ and $r_t := \overline{r}$, we arrive at (44).

Finally, we verify the special structure of the solution function $\tilde{z}$. Let $j \in \{1, \ldots, t\}$ be fixed. Then, we have just shown that $\tilde{z}(r) \in [\beta_{k_j+1}(r), \beta_{k_j}(r)]$ for all $r \in [r_{j-1}, r_j]$. Now, setting

$$\theta_k := \begin{cases} \phi_k, & \text{if } k \leq k_j, \\ -\phi_k, & \text{otherwise}, \end{cases} \quad \bar{w}_k := \begin{cases} w_k + \cdots + w_n, & \text{if } k \leq n, \\ 0, & \text{otherwise}, \end{cases}$$

$$\bar{\mu}_k := \begin{cases} \mu_k + \cdots + \mu_n, & \text{if } k \leq n, \\ 0, & \text{otherwise}, \end{cases}$$

for all $k = 1, \ldots, n+1$, we obtain from (43) that for all $r \in [r_{j-1}, r_j]$

$$0 = \tilde{f}_A(\tilde{z}(r), r) = \sum_{k=1}^{n+1} \theta_k (\beta_k(r) - \tilde{z}(r))^2$$

$$= \sum_{k=1}^{n+1} \left(\theta_k \tilde{z}^2(r) - 2\theta_k(r\bar{w}_k + \bar{\mu}_k)\tilde{z}(r) + \theta_k(r\bar{w}_k + \bar{\mu}_k)^2 \right)$$

$$= (\theta_1 + \cdots + \theta_{n+1})\tilde{z}^2(r) + \ell(r)\tilde{z}(r) + q(r),$$

where the function $\ell(r)$ is affine linear and $q(r)$ is quadratic in r. Both are well-defined by the given parameters. We put $c := \theta_1 + \cdots + \theta_{n+1}$. If $c = 0$, then $\ell(r) \neq 0$ for all $r \in [r_{j-1}, r_j]$. Indeed, otherwise there would exist some $r \in [r_{j-1}, r_j]$ such that $\tilde{z}(r)$ could be chosen arbitrarily (in case that $q(r) = 0$) or such that no value $\tilde{z}(r)$ could be assigned at all (in case that $q(r) \neq 0$). This would contradict the already stated existence and uniqueness of $\tilde{z}(r)$. Hence, the third case of (45) follows. On the other hand, if $c \neq 0$ then the first two cases of (45) come as a consequence of the solution formula for quadratic equations. Here, in order to choose the right out of possibly two solutions, one has to take into account that the function $\tilde{f}_A(\cdot, r)$ is strictly monotonically decreasing for each fixed r (see Proposition 1) and hence, because $\tilde{f}_A(\cdot, r)$ coincides with $c\tilde{z}^2(r) + \ell(r)\tilde{z}(r) + q(r)$ for any fixed $r \in [r_{j-1}, r_j]$, one has to choose the root corresponding to the decreasing branch of that parabola. □

6.2.2 The inner problem

The inner problem consists in finding the representation (40) given the analytic expression for $\tilde{z}$ from the outer problem. This requires first to make explicit the functions h_i from (39). By (31) we have that

$$h_i(r) = \sum_{j=1}^{i} \phi_j |\beta_j(r) - \tilde{z}(r)|^* \quad \forall r \in R_{\text{reg}} \ \forall i = 1, \ldots, n.$$

From (44) and (42) we infer that for all $i = 1, \ldots, n$, for all $j = 1, \ldots, t$ and for all $r \in I_j$:

$$h_i(r) = \sum_{k=1}^{k_j} \phi_k (\beta_k(r) - \tilde{z}(r))^2 - \sum_{k=k_j+1}^{i} \phi_k (\beta_k(r) - \tilde{z}(r))^2.$$

This means that, as a consequence of Theorem 4, the h_i are fully explicitly given on $R_{\text{reg}} = \bigcup_{j=1}^{t} I_j$ via (41) and (45). Since the β_k are affine linear functions, it follows from the representation above that, for each $j \in \{1, \ldots, t\}$, the h_i can be written in the form

$$h_i(r) = \bar{c}_j \tilde{z}(r) + \bar{\ell}_j(r)\tilde{z}(r) + \bar{q}_j(r) \quad \forall r \in R_{\text{reg}},$$

where $\bar{\ell}_j$ and $\bar{q}_j$ are affine linear and quadratic functions, respectively, and $\bar{c}_j$ are some constants. Together with (38) this implies that we can write the feasible region as

$$R_{\text{feas}} = \bigcup_{j=1}^{t} \tilde{I}_j,$$

where

$$\tilde{I}_j := \left\{ r \in I_j \ \middle| \ 0 \leq \bar{c}_j^{(i)} \tilde{z}(r) + \bar{\ell}_j^{(i)}(r)\tilde{z}(r) + \bar{q}_j^{(i)}(r) \quad (i = 1, \ldots, s) \right\}. \quad (48)$$

Here, $\bar{\ell}_j^{(i)}$ and $\bar{q}_j^{(i)}$ are affine linear and quadratic functions, respectively, and $\bar{c}_j^{(i)}$ are some constants. Note, that the index i running from 1 to s represents all inequalities (38) occurring in all cases (i), (ii), (iii). According to (45), the function $\tilde{z}(r)$ can be written as

$$\tilde{z}(r) = \hat{\ell}(r) + \sqrt{\hat{q}(r)}, \quad \tilde{z}(r) = \hat{\ell}(r) - \sqrt{\hat{q}(r)} \quad \text{or} \quad \tilde{z}(r) = \frac{\hat{q}(r)}{\hat{\ell}(r)},$$

respectively, where $\hat{\ell}$ is affine linear and $\hat{q}$ is quadratic in r. With this setting it is easy to see now, that in any case the inequalities in (48) are defined by polynomials of degree 4. The roots of the latter can be determined efficiently. Given these, each of

the single inequalities in (48) is represented by at most three disjoint intervals. Hence, the whole set $\tilde{I}_j$, as a finite intersection of such sets and of the interval I_j, is again a union of finitely many disjoint intervals. Finally, the same holds true for the crucial set R_{feas} which is a finite union of the $\tilde{I}_j$. Summarizing, we may write

$$R_{\text{feas}} = \cup_{j=1}^{l}[a_j, b_j]$$

as a finite union of disjoint intervals with explicitly computed boundaries a_j, b_j. This allows us to compute the χ-probability of this set as

$$\mu_\chi(R_{\text{feas}}) = \sum_{j=1}^{l} \left(F_\chi(b_j) - F_\chi(a_j) \right)$$

by applying an appropriate highly precise numerical approximation of the distribution function of the one-dimensional χ-distribution. In this way, Step 3 of Algorithm 3 may be executed for each given sample $v_i \in \mathbb{S}^{n-1}$.

We note that typically only a few roots of the corresponding polynomials of degree 4 are needed due to Theorem 4, which speeds up the performance considerably.

7 Numerical experiences

In this section we want to test the performance of the presented methodology in the determination of probabilities for feasible exit loads distributed according to a multivariate Gaussian law. We shall compare the spheric-radial decomposition with a generic simulation of Gaussian random vectors. For the sampling on the sphere needed in spheric-radial decomposition we have used the sampling of a standard Gaussian distribution $\mathcal{N}(0, I)$ with posterior normalization. Generic sampling means in contrast the direct simulation of the given normal distribution $\mathcal{N}(\mu, \Sigma)$. In both approaches two different sampling procedures will be applied: the Mersenne-Twister random generator (taken from Boost C++ Libraries) as an advanced Monte Carlo (MC) simulator, and a special Quasi-Monte Carlo (QMC) simulator. The QMC method used in this context is based on digital sequences, namely Sobol' sequences as a special case of low-discrepancy sequences that are included in the category of (t, m, d)-nets and (t, d)-sequences (Dick and Pillichshammer 2010).

In order to guarantee realistic results, we are using modified parameters taken from real low-caloric L-gas and high-caloric H-gas networks of the German gas utility OGE (Open Grid Europe). All computations are performed by C++ implementations on a Linux Sun Station equipped with Intel Xeon CPU @ 2.40GHz.

We start the discussion of numerical results with a test net consisting of a cycle with one entry and 4 exit nodes. Figure 5 shows the network graph and the associated incidence matrix. We assume a homogeneous network in the sense that physical parameters are the same all over the network. In particular, we use lower and upper pressure limits of $p_{\min} = 1.00$ and $p_{\max} = 40.0$, respectively, for every node (entry or exit). A fixed coefficient $\phi = 1.00$ is assigned to all pipes. For the random vector of exit
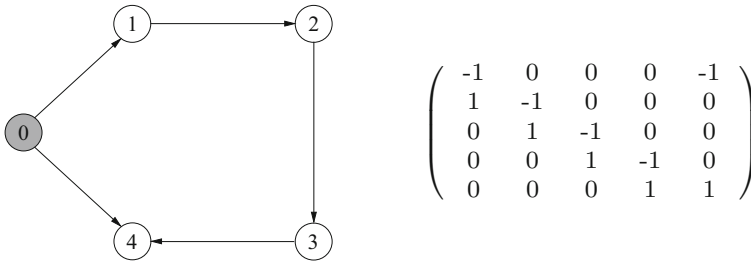
Fig. 5 Network graph and incidence matrix A^+ of the cycle net example

Table 1 Spheric-radial versus generic sampling with 10×1000 samples at cycle net

Sample set	Spheric-Radial		Generic sampling	
	MC (Mersenne)	QMC (Sobol)	MC (Mersenne)	QMC (Sobol)
Series 01	0.981304	0.981442	0.982000	0.982000
Series 02	0.982171	0.981584	0.973000	0.981000
Series 03	0.980530	0.981083	0.977000	0.982000
Series 04	0.981335	0.981639	0.981000	0.981000
Series 05	0.980645	0.981593	0.990000	0.979000
Series 06	0.980313	0.981420	0.988000	0.985000
Series 07	0.981934	0.981634	0.982000	0.981000
Series 08	0.981119	0.981890	0.977000	0.984000
Series 09	0.982377	0.981145	0.982000	0.980000
Series 10	0.981932	0.981631	0.979000	0.984000
Mean Probability	0.981366	0.981506	0.9811	0.9819
Variance	5.2294e−07	5.9061e−08	2.5878e−05	3.6556e−06
SD	7.2315e−04	2.4302e−04	5.0870e−03	1.9120e−03
Time (s)	0.41	0.57	0.29	0.44
Efficiency	35.00	222.97	1.00	4.67

load nominations we prescribe a multivariate Gaussian distribution. The parameters of this distribution are inspired by the statistical analysis of real load data as described in Koch et al. (2015, Chapter 13).

Table 1 collects the result of numerical computations for 10 test series of 1000 samples each. We observe for both sampling schemes (MC and QMC) a substantial variance reduction by a factor of approximately 50 when applying the spheric-radial decomposition. Due to a larger numerical effort, the computing times for the spheric-radial decomposition slightly increase. For a fair comparison between different methods taking into account the obtained precision (variance) of the result and the needed numerical effort (computing time) we resort to the concept of efficiency as in Deák (2000, p. 112):
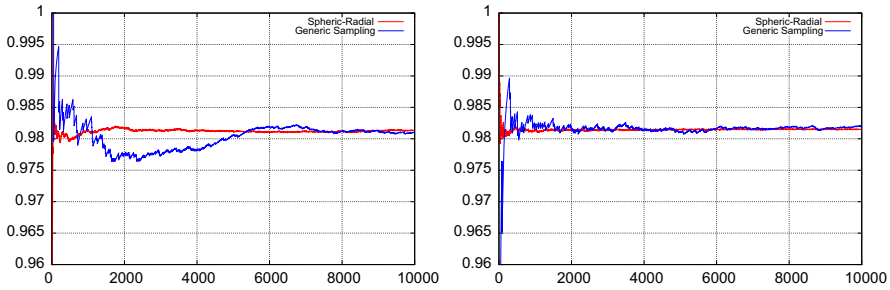
Fig. 6 Moving average of computed probability with respect to sample size for Mersenne Twister (*left*) and QMC sampling (*right*)

Method 2 with variance σ_2^2 and computing time t_2 is said to have efficieny $(\sigma_1^2 t_1)/(\sigma_2^2 t_2)$ with respect to Method 1 with variance σ_1^2 and computing time t_1.

This notion is certainly inspired by the well-known fact that in MC simulation the decrease in variance is proportional to the increase in the sample size needed. In Table 1 efficiencies are indicated relative to generic MC sampling, the method with poorest performance. Both effects of improvement (use of QMC rather than MC and use of spheric-radial decomposition rather than generic sampling) are clearly recognized.

Figure 6 displays the curves of estimated probability for an increasing sample size. It shows the moving average of the probability for sample sizes listed at the abscissa. The left picture plots the results for spheric-radial decomposition and generic sampling when using Mersenne Twister, the second one plots the same for QMC. In both cases, spheric-radial decomposition yields a much faster stabilization of results than generic sampling and again the effect is enhanced by applying QMC rather than MC.

Finally, we consider the example of two regular trees of different sizes. Both are single entry nets, where the entry is located at the root of each tree. All remaining nodes of the trees are assumed to be exit nodes. As before, we deal with a homogeneous network and we use the same general physical parameters as quoted in the previous example. The goal of this test series is to investigate the performance of the spheric-radial decomposition approach, even for large sizes. In example (a) we consider a number of 4 stages with branching degree 3, which leads to a tree containing a number of overall 121 nodes. In example (b) we consider 3 stages and branching degree 5, such that the tree consists of 156 nodes including the entry node. Table 2 summarizes the numerical results for both examples. It turns out that the computation time increases reasonably due to the larger size of the networks. In particular, to compute all intervals M_i in (22), the number of inequalities to be evaluated increases quadratically with the number of nodes. In the tree examples we only focus on the best performing method, namely spheric-radial decomposition along with QMC sampling. To realize a proper estimation for both, mean and variance of the probability to be determined we generated as before 10 test series of 1000 samples. It turns out that for higher dimension the variance reduction effect of spheric-radial decomposition is less significant, but, it is still noticeable. Indeed, the variance of generic sampling can never be less than that

Table 2 Numerical results for both regular tree examples and applying the spheric-radial decomposition together with QMC sampling for 10×1000 sample size

	Tree example (a)	Tree example (b)
Nodes	121	156
Degree	3	5
Stages	4	3
Mean probability	0.68004	0.71367
Variance	4.3668e−05	4.6478e−05
SD	6.6082e−03	6.8175e−03
Time (s)	88.3	135.6

of spheric-radial decomposition (Ackooij and Henrion 2014, p. 2). In our examples the probability is approximately $p \approx 0.70$ and we used a sample size of $N = 1000$. For Monte Carlo sampling it is known that the theoretical variance for computing the probabilty p with sample size N is $N^{-1}(p - p^2)$. Hence, in the examples the theoretical variance of generic Monte Carlo is approximately 2.1×10^{-4}, which is certainly higher than observed for the spheric-radial decomposition.

8 Optimization problems with probabilistic constraints

In this paper we have focused on computing the probability of the set M of technically feasible exit load vectors as defined in (20) via the set $\tilde{M}$ characterized in Theorem 1. While a mere computation of such probabilities is already of much importance, for instance in the *verification of booked capacities* (see Introduction), it forms the basis as well for more demanding problems in which these probabilities depend on parameters to be optimized according to some cost function. Such parameters occur in Theorem 1 as lower and upper pressure bounds p^{min}, p^{max} or as coefficients Φ. Though we were keeping these parameters fixed in our analysis, one could also understand them as decision variables. For instance, in a design phase for a network of given topology, one might be interested in installing material-dependent upper pressure bounds which are cost-minimal on the one hand and which still guarantee that exit loads are feasible at a specified probability level. Formalizing this idea, the set of feasible exit loads colud be denoted now by $M(p^{max})$ in order to emphasize the dependence of M on the upper pressure bounds. One then would solve an optimization problem of the type

$$\min \left\{ c^T p^{max} \mid \mathbb{P}(\xi \in M(p^{max})) \geq p \right\}.$$

Here, c denotes a cost vector associated with the material needed to guarantee the desired upper pressure bounds in the nodes of the network. As before, ξ refers to the random vector of exit loads and $p \in [0, 1]$ is a specified probability level to satisfy these loads (e.g., $p = 0.95$). The inequality defining the constraint for the decision vector p^{max} in this optimization problem is called a *probabilistic constraint* (see, e.g., Prékopa 1995; Shapiro et al. 2009). For the numerical solution of such optimization problems with probabilistic constraints it is crucial not only efficiently

to determine the probabilities associated with some fixed decision vector but also their gradients. Interestingly, the spheric-radial decomposition approach applied in this paper admits the computation of this gradient in the same sampling framework used for the probabilities themselves. More precisely, the time-consuming Step 2. of Algorithm 3 yielding a representation of the sets M_i as a union of finitely many disjoint intervals has to be carried out only once per sample and can be exploited then not only for updating the probabilities but even their partial derivatives (with respect to the decision vector) at the same time. In this way, the computation of partial derivatives almost comes for free. This effect which is based on a gradient formula presented in Ackooij and Henrion (2014) enhances the significance of the spheric-radial decomposition approach.

We emphasize that the methodology presented here does not restrict to a single tree or a single cycle but is easily formulated for more general networks as long as cycles are node-disjoint, and then possibly several separated trees attached to the cycles.

References

Ahuja RK, Magnanti TL, Orlin JB (1993) Network flows. Prentice Hall, New Jersey

Bertsimas D, Tsitsiklis JN (1997) Introduction to linear optimzation. Athena Scientific, Belmont

Brauchart JS, Saff EB, Sloan IH, Womersley RS (2014) QMC designs: optimal order Quasi Monte Carlo integration schemes on the sphere. Math Comput 83:2821–2851

Deák I (2000) Subroutines for Computing normal probabilities of sets—computer experiences. Ann Oper Res 100:103–122

Dick J, Pillichshammer F (2010) Digital nets and sequences: discrepancy theory and Quasi-Monte Carlo integration. Cambridge University Press, Cambridge

Dvijotham K, Vuffray M, Misra S, Chertkov M (2015) Natural gas flow solutions with guarantees: a monotone operator theory approach. Cornell University Library. arXiv:1506.06075v1

Fügenschuh A, Geissler B, Gollmer R, Hayn C, Henrion R, Hiller B, Humpola J, Koch T, Lehmann T, Martin A, Mirkov R, Römisch W, Rövekamp J, Schewe L, Schmidt M, Schultz R, Schwarz R, Schweiger J, Stangl C, Steinbach M, Willert B (2014) Mathematical optimization for challenging network planning problems in unbundled liberalized gas markets. Energy Syst 5:449–473

Genz A, Bretz F (2009) Computation of multivariatenormal and t probabilities (Lecture notes in statistics), vol 195. Springer, Heidelberg

Kirchhoff G (1847) Über die Auflösung der Gleichungen, auf welche man bei der Untersuchung der linearen Verteilung galvanischer Ströme geführt wird. Ann Phys Chem 12:497–508

Koch T, Hiller B, Pfetsch M, Schewe L (eds) (2015) Evaluating gas network capacities. MOS-SIAM Series on optimization, vol 21

Misra S, Vuffray M, Chertkov M (2015) Maximum throughput problem in dissipative flow networks with application to natural gas systems. Cornell University Library. arXiv:1504.02370v1

Osiadacz A (1987) Simulation and analysis of gas networks. Gulf Publishing Company, Houston

Pfetsch M, Fügenschuh A, Geissler B, Geissler N, Gollmer R, Hiller B, Humpola J, Koch T, Lehmann T, Martin A, Morsi A, Rövekamp J, Schewe L, Schmidt M, Schultz R, Schwarz R, Schweiger J, Stangl C, Steinbach M, Vigerske S, Willert B (2015) Validation of nominations in gas network optimization: models, methods, and solutions. Optim Methods and Softw 30:15–53

Prékopa A (1995) Stochastic programming. Kluwer, Dordrecht

Ríos-Mercado RZ, Boras-Sánchez C (2015) Optimization problems in natural gas transportation systems: a state-of-the-art review. Appl Energy 147:536–555

Ríos-Mercado RZ, Wu S, Boyd EA, Scott LR (2000) Model relaxations for the fuel cost minimization of steady-state gas pipeline networks. Math Comput Model 31:197–220

Shapiro A, Dentcheva D, Ruszczyński A (2009) Lectures on stochastic programming. MPS-SIAM series on optimization, vol 9

Stangl C (2014) Modelle, Strukturen und Algorithmen für stationäre Flüsse in Gasnetzen. Dissertation, Fakultät für Mathematik, Universität Duisburg-Essen

Van Ackooij W, Henrion R (2014) Gradient formulae for nonlinear probabilistic constraints with Gaussian and Gaussian-like distributions. SIAM J Optim 24:1864–1889

Vuffray M, Misra S, Chertkov M (2015) Monotonicity of dissipative flow networks renders robust maximum profit problem tractable:general analysis and application to natural gas flow. Cornell University Library. arXiv:1504.000910v1

Wong P, Larson R (1968) Optimization of natural gas pipeline systems via dynamic programming. IEEE Trans Autom Control 13:475–481

Zucker RD, Biblarz B (2002) Fundamentals of gas dynamics, 2nd edn. Wiley, Hoboken